



# Deep soil water $^{18}\text{O}$ and $^2\text{H}$ measurements preserve long term evaporation rates on China's Loess Plateau

Wei Xiang<sup>1</sup>, Bingcheng Si<sup>1,2</sup>, Min Li<sup>1</sup>, Han Li<sup>1</sup>

<sup>1</sup> Key Laboratory of Agricultural Soil and Water Engineering in Arid and Semiarid Areas, Ministry of Education, Northwest A&F University, Yangling, Shaanxi Province, 712100, China

<sup>2</sup> Department of Soil Science, University of Saskatchewan, Saskatoon, SK, Canada

Correspondence to: Bingcheng Si (Bing.Si@usask.ca)

**Abstract.** Knowledge about the long-term average soil evaporation, especially the ratio of evaporation to precipitation ( $f$ ), is important for assessing the total available water resources. However, determining the long-term  $f$  remains technically challenging because soil evaporation is highly dynamic. Here we hypothesize that the stable isotopes ( $^2\text{H}$  and  $^{18}\text{O}$ ) of deep soil water preserve the long-term evaporation effects on precipitation and can be used to estimate long-term  $f$ . Our results showed that the deep soil water (2 - 10 m) had a mean line-conditioned excess (lc-excess) less than zero (-13.1‰ to -3.8‰) at the 15 sites across China's Loess Plateau, suggesting that evaporation effects are preserved in the isotopic compositions of the deep soil water. We then estimated  $f$  by the new lc-excess method that combines lc-excess and the Rayleigh fractionation theory, because it does not require the initial source isotopic values of soil water, which has a distinct advantage over traditional isotope-based methods (e.g. Craig-Gordon model) that require such information a priori. The estimated  $f$  of the 15 sites varied from 11% to 30%, and over 60% of the variability of  $f$  was explained by the well-known Budyko dryness index. These data are also comparable with available annual estimates under similar climate regions of the world. Furthermore, these data represent a long-term average value because soil water tritium profile shows that deep soil water has a long residence time on the order of years to decades. Our work suggests that isotopic compositions of deep soil water can be used to calculate long-term average  $f$  where water flow within the unsaturated zone is piston-like flow predominantly, and the new lc-excess method provides an effective tool to estimate  $f$ .



## 1 Introduction

Water loss from soil by evaporation is an essential component of the terrestrial water cycle (Or and Lehmann, 2019). Estimation of soil evaporation, not only the amount but also the ratios of it to precipitation ( $f$ ) or evapotranspiration, within the different landscapes helps understanding ecohydrological processes (Sprenger et al., 2017b; Sprenger et al., 2017a), quantifying the water balance (Skrzypek et al., 2015), partitioning evapotranspiration (Anderson et al., 2017; Kool et al., 2014), and calibrating rainfall-runoff models (Birkel et al., 2014). Because of the dynamic nature due to variation of climate, surface soil water capacity, and vegetation conditions (Or and Lehmann, 2019), a more reliable assessment of soil evaporation or  $f$  needs to determine the long-term average values (Stoy et al., 2019), which remains a serious technical constraint (Kool et al., 2014).

Many methods have been developed for measuring soil evaporation, and thus estimating  $f$  by combining soil evaporation measurements with climate record (i.e. precipitation). The field measurement methods, such as micro-lysimeters, soil heat pulses, chambers, micro Bowen ratio energy balance, and eddy covariance (Kool et al., 2014), only estimate soil evaporation at particular points and have relative short observational timescales (days to growing season) (Anderson et al., 2017). Temporally integrating these estimates needs high-frequency continuous observations in-situ, which is time-consuming and costly. Notwithstanding modeling is useful for estimating soil evaporation over relatively long periods, current models are rarely capable of estimating under-canopy evaporation (Good et al., 2015) and even when they are, they tend to overestimate the soil evaporation and need to be validated by long-term field measurements (Lian et al., 2018; Niu et al., 2019).

Conversely, a relatively long-term  $f$  can be estimated using stable  $^2\text{H}$  and  $^{18}\text{O}$  isotopes, because they are only enriched during soil evaporation processes (Zimmermann et al., 1966) and can integrate soil evaporation processes occurring over interest of period (Jasechko et al., 2013; Allison and Barnes, 1983). The primary advantage is that it does not need continuous field observations with high frequency and have been used to estimate  $f$  in various studies (Allison and Barnes, 1983; Sprenger et al., 2017a; Hsieh et al., 1998; Mahindawansa et al., 2019). Previous studies commonly utilize the shallow soil water  $^2\text{H} / ^{18}\text{O}$  isotopes; however, obtaining long-term average  $f$  requires continuous sampling effort of shallow soil due to the strong isotopic dynamics in that part of the soil profile, which can be costly. Precipitation falling as rainfall on



the land surface undergoes a series of processes including evaporation in the canopy and the soil surface (isotope fractionation), transpiration within root zone (isotope non-fractionation), and mixing in the shallow soil, and eventually infiltrates to the deeper soil and groundwater or forms runoff down slope to a stream (Good et al., 2015). Therefore, deep soil water isotopic compositions may serve as an ideal logger of surface soil evaporation, preserving the effects of evaporation on precipitation over a relatively long period (DePaolo et al., 2004; Sprenger et al., 2016). Deep soil water could provide an opportunity to estimate the long-term average  $f$ , but the opportunity has not been systematically explored.

Methods to determine  $f$  from isotopic composition of water are generally based on the well-known Craig-Gordon model by single-isotope system ( $^{18}\text{O}$  or  $^2\text{H}$ ) (Craig and Gordon, 1965); however, estimates from  $^{18}\text{O}$  are often inconsistent with those from  $^2\text{H}$  (Sprenger et al., 2017a; Mahindawansa et al., 2019). The dual-isotope systems, including the deuterium-excess (d-excess, as defined by Dansgaard (1964)) and the line-conditioned excess (lc-excess, Landwehr and Coplen (2006)), overcome the inconsistency, but are often used as a qualitative indicator of evaporation intensity rather than quantitatively. That is, the d-excess or lc-excess of a water sample, display the degree of evaporation that the water experienced only; but the fraction of evaporation loss to the initial water body (i.e.  $f$ ) can not be determined by d-excess or lc-excess. Recent works suggest that combining d-excess and the Rayleigh fractionation theory (Clark and Fritz, 1997) can estimate  $f$  quantitatively and is shown to be more robust than the traditional Craig-Gordon method (Hu et al., 2018; Zhao et al., 2018). However, a key problem is that the d-excess is not only an indicator of evaporation but also reflects both the original source of water vapor and of relative humidity in the source area (Masson-Delmotte et al., 2005). Conversely, lc-excess defines the offset of a water sample to its Local Meteoric Water Line (LMWL) due to kinetic fractionation caused by evaporation only (Sprenger et al., 2017b). But to the best of our knowledge, little is known about the performance of lc-excess on quantifying  $f$ .

Therefore, the overall objective of this study was to estimate long-term  $f$  quantitatively by combining deep soil water isotopic compositions and lc-excess, based on the deep soil water isotopic compositions measurement at multiple sites on China's Loess Plateau. Specifically, we ask the following questions: (i) Can we use deep soil water isotopic compositions to estimate soil evaporation to precipitation ratio? and (ii) How to use lc-excess in estimating evaporation to precipitation



ratio?

## 2 Materials and methods

### 2.1 Study site

China's Loess Plateau, located in northern China, is the largest loess deposit in the world, with a mean thickness of 100 m and the maximum thickness of up to ~350 m (Zhu et al., 2018). Loess is quaternary sediment and is marked by three layers: the upper Late Pleistocene Malan Loess, the middle Middle Pleistocene Lishi Loess, and the lower Early Pleistocene Wu-cheng Loess (Liu, 1985). This region is characterized by a warm temperate continental monsoon climate, with the mean annual precipitation, potential evapotranspiration (Penman, 1948), and temperature of 200-900 mm, 700-1400 mm, and 8-14°C, respectively (Fig. 1). The groundwater level is 50-100 m below the land surface.

### 2.2 Sampling and measurement

We obtained a total of 15 deep soil cores under different climate regions (Fig. 1d; Table 1): 12 soil cores (S1-7 and S9-13) were sampled over the period 2015-2019, and the remaining cores (S8 and S14-15) collected from the literature where deep soil water isotope information was available. The vegetation of the sampling sites is farmland and grassland. The farmland was characterized by long-term (more than 100-year-old) rain-fed winter wheat or summer maize, and the grasslands were converted from farmlands. All of the above soil sites are located at a very flat landscape where runoff is often negligible.

In order to assess the vertical distribution of soil water isotopic composition, a hand auger with stem extension was used at each site to obtain samples at an interval of 0.2 m to a depth of 9-10 m. Each soil sample was stored in a 250 mL plastic bottle sealed with parafilm, transported to the laboratory and stored in the refrigerator at -20 °C prior to soil water extraction. Further, to assess the temporal variability of soil water isotopic composition, we collected eight 5-m soil cores beneath a 13-year-old apple orchard (converted from farmland, < 200 m away from the farmland) at site S11 during 2015-2016 (collected on 2015/7/12, 2015/8/19, 2016/3/20, 2016/5/30, 2016/7/3, 2016/7/30, 2016/8/30, and 2016/10/15).



Soil water was extracted via the cryogenic vacuum distillation method (Orlowski et al., 2016), and the water extraction and collection efficiencies both ranged from 98% to 102% for each sample. The extracted water was then stored in a 10 mL glass bottle and kept in the refrigerator at 4 °C before stable isotope analysis. The stable isotopic compositions (<sup>18</sup>O and <sup>2</sup>H) of soil water samples were determined with an isotopic liquid water analyzer (LGR LIWA 45EP, USA), and the isotopic values are presented using the delta notation (in ‰):

$$\delta_{sample} = \left( \frac{R_{sample}}{R_{VSMOW}} - 1 \right) \times 1000 \quad (1)$$

where the  $R_{sample}$  and  $R_{VSMOW}$  are the <sup>2</sup>H/<sup>1</sup>H (<sup>18</sup>O/<sup>16</sup>O) ratio of sample and Vienna Standard Mean Ocean Water (VSMOW), respectively. The precision of the isotopic measurements was 1.0‰ and 0.2‰ for δ<sup>2</sup>H and δ<sup>18</sup>O, respectively.

## 2.3 Theory and methods

### 2.3.1 Lc-excess

Landwehr and Coplen (2006) specified that the offset of a water sample from the LMWL is the lc-excess:

$$lc - excess = \delta^2H - a\delta^{18}O - b \quad (2)$$

where the  $a$  and  $b$  are the slope and intercept of LMWL, respectively. Precipitation samples that have undergone minimal to no evaporation prior to sample collection would have, by definition, an lc-excess of zero. A negative lc-excess value that is smaller than one negative standard deviation of the precipitation suggests that a water sample has undergone some evaporative isotopic enrichment. The smaller the lc-excess value, the stronger the influence of evaporation. Therefore, we used the lc-excess as a qualitative indicator of the evaporation to precipitation ratio.

We obtained long-term precipitation isotopic data from the International Atomic Energy Agency (IAEA) Global Network of Isotopes in Precipitation from five stations located in Zhengzhou, Taiyuan, Baotou, Xi'an, and Lanzhou (**Fig. 1d**). Based on the δ<sup>2</sup>H and δ<sup>18</sup>O of all monthly precipitation samples ( $n = 212$ ), the regional LMWL was determined using the least square regression weighted by precipitation amount:  $\delta^2H = 6.89 (0.15) \delta^{18}O - 0.16 (1.23)$ ,  $R^2 = 0.91$ , which was used as the reference line for all soil sites.



115 **2.3.2 Estimation of evaporation to precipitation ratio**

Precipitation water entering the soil may be partially evaporated gradually, and the water remaining in the soil will thus be enriched in heavy isotopes ( $^{18}\text{O}$  and  $^2\text{H}$ ) by evaporation fractionation (Sprenger et al., 2016). Assuming that soil water evaporation follows the Rayleigh fractionation theory (Clark and Fritz, 1997), the evaporation to precipitation ratio  $f$  of a sampled soil water after evaporation can be written as:

120 
$$R_s = R_0(1 - f)^{(\alpha-1)} \quad (3)$$

where  $\alpha$  is a fractionation factor, and  $R_s$  and  $R_0$  are the  $^2\text{H}/^1\text{H}$  (or  $^{18}\text{O}/^{16}\text{O}$ ) ratio of the evaporated water sample and its initial water source, respectively. Based on Eqs. (1) and (3), we used  $\delta_{(s)}$  to replace the  $R_{(s)}$ , and then Eq. (3) can be written as:

$$\delta_0 = (\delta_s + 1000)(1 - f)^{(1-\alpha)} - 1000 \quad (4)$$

125 where  $\delta_s$  and  $\delta_0$  are the isotopic values of the evaporated water sample and the initial water source, respectively. Combining Eqs. (2) with (4), we obtain:

$$lc_0 = \frac{[\delta^{2H_s} + 1000]}{(1-f)^{[\alpha^{(2H)} - 1]}} - \frac{a(\delta^{18O_s} + 1000)}{(1-f)^{[\alpha^{(18O)} - 1]}} + 1000(a - 1) - b \quad (5)$$

130 where  $lc_0$  is the lc-excess value of the initial water source.  $\delta^{2H_s}$  and  $\delta^{18O_s}$  are the isotopic compositions of an evaporated water sample.  $\alpha_{(s)}$  is a fractionation factor that reflects both the equilibrium fractionation ( $\alpha^*_{(s)}$ ) and the kinetic enrichment ( $\varepsilon_{k(s)}$ ) factors ( $\alpha_{(s)} = \frac{1}{\alpha^*_{(s)} + \varepsilon_{k(s)}}$ ) (Clark and Fritz, 1997). The  $\alpha^*_{(s)}$  is a function of temperature ( $T$ ) in degrees Kelvin (Eqs. (6) and (7)) (Gonfiantini, 1986; Majoube, 1971), and the  $\varepsilon_{k(s)}$  is related to relative humidity ( $Rh$ ) (Eqs. (8) and (9)) (Horita et al., 2008; Benettin et al., 2018):

$$\ln [\alpha^*_{(2H)}] = \frac{24.844}{T^2}(10^3) - \frac{76.248}{T} + 52.612(10^{-3}) \quad (6)$$

$$\ln [\alpha^*_{(18O)}] = \frac{1.137}{T^2}(10^3) - \frac{0.4156}{T} - 2.0667(10^{-3}) \quad (7)$$

$$\varepsilon_{k(2H)} = n(1 - Rh)(1 - 0.9755) \quad (8)$$

135 
$$\varepsilon_{k(18O)} = n(1 - Rh)(1 - 0.9723) \quad (9)$$

where the parameter  $n$  accounts for the aerodynamic regime above the evaporating liquid-vapor interface, which ranges from 0.5 (saturated soil condition) to 1.0 (very dry soil condition). We set  $n$  to 0.75 because the evaporating soil layer was



140 expected to the alternation of saturating and drying over time (Benettin et al., 2018). We estimated the monthly  $\alpha_{k(t)}$  and  $\varepsilon_{k(t)}$  using monthly temperature and relative humidity, and then the annual values are estimated by summation of the monthly values weighted by the monthly temperature and relative humidity. If  $\alpha_{k(t)}$  and  $\varepsilon_{k(t)}$  are calculated, the long-term mean annual  $\alpha_{(t)}$  can be determined. For each soil site, the long-term (1981-2010) mean monthly temperature and relative humidity data were obtained from the nearby meteorological station (**Fig. 1**).

145 The  $lc_0$  was set to zero because we assumed that soil water at our study sites only originates from the local precipitation over a long time (Cheng et al., 2014). If the isotopic composition of soil water ( $\delta^2\text{H}_s$  and  $\delta^{18}\text{O}_s$ ), the slope ( $a$ ) and intercept ( $b$ ) of LWML, and climate parameters ( $T$  and  $Rh$ ) are all known, the  $f$  can be calculated from Eqs. (5) to (9). In the Eq. (5), the uncertainties resulting from the calculation of  $\alpha_{(t)}$  can be ignored because the multi-year mean monthly temperature and relative humidity are used (Zhao et al., 2018). Therefore, the main sources of uncertainty for  $f(S_f)$  are from the measured isotopic compositions of deep soil water (2-10 m), and slope ( $a$ ) and intercept ( $b$ ) of LMWL. If  $x = \delta^2\text{H}_s$  and  $y = \delta^{18}\text{O}_s$ ,  $S_f$  can be estimated based on the first-order perturbation analysis:

150 
$$(S_f)^2 = \left(\frac{\partial f}{\partial x}\right)^2 \cdot (S_x)^2 + \left(\frac{\partial f}{\partial y}\right)^2 \cdot (S_y)^2 + \left(\frac{\partial f}{\partial a}\right)^2 \cdot (S_a)^2 + \left(\frac{\partial f}{\partial b}\right)^2 \cdot (S_b)^2 \quad (10)$$

where the  $S_{(j)}$  represents the standard error of the relevant variable and the  $\frac{\partial f}{\partial (j)}$  represents the partial derivative of  $f$  with respect to the relevant variable.

### 3 Results

#### 3.1 Stable isotopic compositions of soil water

155 **Figure 2** shows the vertical fluctuations and temporal variations of soil water isotopic compositions at different depths at site S11. Generally, the  $\delta^2\text{H}$  and  $\delta^{18}\text{O}$  of soil water changed with depth, but shallow soil (0-2 m) displayed more fluctuations along with depth than deep soil ( $> 2$  m). For example, the  $\delta^2\text{H}$  value varied from -77.2 ‰ to -23.1 ‰ in the top 2 m, but only from -71.5 ‰ to -64.8 ‰ at depth  $> 2$  m. Similarly, the temporal variability of soil water isotope composition at S11 was the largest in the surface soil and gradually weakened with increasing depth and became stable below 2.0 m.



160 Therefore, both the vertical fluctuations and temporal variability at S11 suggested that soil water isotopic compositions were stabilized below 2.0 m. Further, despite of differences among the sites, all the 15 deep profiles showed that soil water isotopic compositions were stabilized with depth below 2 m (**Fig. 3**).

The mean lc-excess values of deep soil water (> 2 m) for the 15 sites ranged from -13.1‰ to -3.8‰, and was significantly less than that of precipitation ( $p < 0.05$ ) (**Fig. 4**). For all sites, the lc-excess difference between deep soil water and precipi-  
165 tation were larger than that of the measurement error (1.02‰). Thus, these suggested that deep soil water isotopes preserve obvious isotope fractionation signatures. Furthermore, deep soil water lc-excess values differed significantly among sites ( $p < 0.05$ ). This reflects the difference in evaporation intensity among sites. For instance, the S8 had the smallest mean lc-excess (-13.1‰) while S6 had the largest value (-3.8‰), suggesting that evaporation intensity at S8 was stronger than that at S6.

### 170 **3.2 Estimation of evaporation to precipitation ratio**

We used deep soil water isotopic compositions and estimated evaporation to precipitation ratio ( $f$ ) for each site using Eq. (5) and the associated uncertainty calculated using Eq. (12) (**Fig. 5a**). The resulting  $f$  differed among sites and varied from 11% to 30%, with an average of 21% and a standard deviation of 6%. The uncertainty is relatively small, being within the range of 2.5% - 8.7%. Moreover, the  $f$  values had a strong negative linear relationship with the deep soil water lc-excess ( $f$   
175 =  $-2.086lc\text{-excess} + 4.086$ ,  $R^2 = 0.81$ ,  $p < 0.001$ ). This is reasonable because the lc-excess is a qualitative index of evaporation intensity, and the more intense evaporation the water experiences, the lower the lc-excess and the larger the  $f$ .

Both the  $f$  and lc-excess were poorly correlated to the mean annual potential evapotranspiration ( $R^2 = 0.04$  for lc-excess;  $R^2 = 0.01$  for  $f$ ) (**Fig. 5b**). But they were strongly statistically significantly correlated with the mean annual precipitation ( $R^2 = 0.68$  and  $p < 0.05$  for lc-excess;  $R^2 = 0.67$  and  $p < 0.001$  for  $f$ ) (**Fig. 5c**) and the Budyko dryness index ( $R^2 = 0.74$  and  
180  $p < 0.001$  for lc-excess;  $R^2 = 0.63$   $p < 0.001$  for  $f$ ) (**Fig. 5d**). This indicates that evaporation intensity at our study sites is closely correlated to the precipitation and dryness index rather than the potential evapotranspiration.





## 4 Discussion

### 4.1 Why deep soil water isotope preserves soil evaporation effects?

Soil evaporation is a major factor for isotope enrichment of infiltration precipitation; however, it exponentially decreased  
185 with soil depth (Zimmermann et al., 1966; Allison and Barnes, 1983), resulting in obvious isotope fractionation signatures  
within a few centimeters to dozens of centimeters of shallow soil layers only (Sprenger et al., 2016). Here, we showed that  
deep soil water isotopic compositions (2 - 10 m) from all sites on China's Loess Plateau indeed preserve the obvious iso-  
tope fractionation signatures, as evidenced from the negative  $\delta$ -excess values (**Fig. 4**). However, the isotope fractionation  
signatures of deep soil water cannot be attributed directly to surface soil evaporation at the current condition because of the  
190 thick soil depths. Nevertheless, this is consistent with many studies that also detected isotopic fractionation signals in deep  
soil (DePaolo et al., 2004; Evaristo et al., 2016; Allison and Hughes, 1983; Fontes et al., 1986). For instance, Evaristo et al.  
(2016) showed that evaporative isotopic enrichment either did not systematically decrease with depth or that evaporation  
was restricted to the top 10 cm and transported vertically with depth.

What are the mechanisms that lead to the relative  $^2\text{H}$  and  $^{18}\text{O}$  enriched in deep soil water? As is well known, precipitation  
195 infiltration and subsequent downward percolation within soils is often described as two end-member scenarios: piston flow  
and preferential flow (Gazis and Feng, 2004). In piston flow mode, water from more recent precipitation forces the older  
soil water to flow down. Under such scenario, deep soil water most likely originated from a mixture of precipitation waters  
that underwent variable degrees of evaporation within the shallow layers and then moved down to these depths and thus  
isotopic fractionation signal in deep soil is possible. In preferential flow mode, water bypass soil matrix and directly infil-  
200 trated into the deep soil. Thus, deep soil water will not show obvious isotopic fractionation signals. Given that the nature of  
these two flows coexist within filed soils (Lin, 2010) and their proportions (piston flow vs preferential flow) depending on  
local soil characteristics (Gazis and Feng, 2004), deep soil water would show obvious isotopic fractionation signals when  
piston flow is not negligible.

On China's Loess Plateau, numerous works showed that piston flow is the dominant flow within the deep unsaturated zone  
205 (Lin and Wei, 2006; Zhang et al., 2017; Zheng et al., 2017; Yang and Fu, 2017; Huang et al., 2019; Li et al., 2019). Thus, deep



soil water would originate from above water that experienced soil evaporation and then moved into these depths by piston flow, and thus the observed isotopic fractionation within deep soil would be reasonable and can be attributed to historic evaporation. Therefore, the soil profile can be divided into mixing and stabilized zones (**Fig. 2c**). Isotopic compositions of mixing zone or deep soils may reflect the integrated influence of evaporation on precipitation water. Therefore, deep soil water isotopic compositions may indeed be used for the estimation of evaporation to precipitation ratio.

#### 4.2 What is the timescale of our $f$ estimates based on deep soil water isotopes?

The stable isotopic compositions of soil water stabilized below approximately 2.0 m, for all of the 15 sites (**Fig. 2 and 3**). Precipitation and soil evaporation are two main factors to the variation of soil water isotopes; however, soil evaporation is limited to a few to dozens of centimeters only (Cheng et al., 2014) and precipitation infiltration depth rarely exceeds two meters at our study area (Jin et al., 2018; Zhao et al., 2019). Therefore, the invariable isotope compositions of deep soil water indicate that deep soil water is free of seasonal variation in evaporation and precipitation infiltration (Thomas et al., 2013; Sprenger et al., 2016; Cheng et al., 2014). This is consistent with previous isotope studies (Wan and Liu, 2016; Yang and Fu, 2017) and is supported by the observation of soil water dynamics in this region (Zhao et al., 2019). Moreover, the reduced variations of stable isotopes in deep soils can be attributed to the mixing processes in the deep unsaturated zone since it has the long residence time (DePaolo et al., 2004; Thomas et al., 2013).

A clearly-identifiable tritium peak corresponding to a 1963 precipitation input peak is located at the depth of 6.1 m at S11 (**Fig. 2c**) and 9.8 m at S7 (Li and Si, 2018). Thus, the pore water velocities were 11 and 17 cm yr<sup>-1</sup> at S11 and S7, respectively. This suggests that that deep soil water (2 - 10 m) would have a relatively long residence time that ranges from 12 to 90 years. Thus, the  $f$  obtained from the average deep soil water isotopic compositions had a mean residence time of about 51 years.

The time scales considered in traditional field evaporation measurement (e.g. micro-lysimeter, and soil heat pulse) range from minutes to growing seasons (Kool et al., 2014; Anderson et al., 2017). Annual evaporation may be obtained from Eddy covariance technology, but those measurements are only available over a time span of ~ 10 years, at only dozens of sites across the world (Scott and Biederman, 2017; Gu et al., 2018). Evaporation obtained from the isotopes of groundwater



230 or lake water may also have long residence time like deep soil water (Jasechko et al., 2013;Zhao et al., 2018), but there are cases where the expression of isotopic fractionation signature in groundwater is modulated by the variable connectivity between mobile and immobile soil water pools (Good et al., 2015), and groundwater may be much older, and could well represent conditions far different from the current surface vegetation and climate conditions (Jasechko et al., 2017). Therefore, relative to groundwater, deep soil water is more representative of evaporation.

235 Our work shows that deep soil water isotopic compositions offer an effective tool to estimate the long-term average  $f$ , complementing other field measurements. However, we identified deep soil as soil at a depth greater than 2.0 m in this study. Sprenger et al. (2016) reported a depth of 0.3 m in the temperate regions, 0.5 m in the Mediterranean climate, and 3.0 m in the arid regions. Deep soil is common in many regions of the world (Xu and Liu, 2017), especially in arid and semiarid regions; its water isotopic compositions may become more readily available as isotope analyzers become more  
240 accessible (Sprenger et al., 2015). Therefore, deep isotopic compositions of soil water have the potential to be widely used to estimate long-term  $f$ .

Additionally, once the long-term  $f$  values were estimated, the long-term transpiration to evapotranspiration fraction can be estimated with the help of measurement methods (e.g. water balance, eddy covariance, and sap flow) (Kool et al., 2014). The information can help the state-of-art models to improve the accuracy of evapotranspiration partitioning (Lian et al.,  
245 2018;Niu et al., 2019).

#### 4.3 Is it reliable to use deep soil water isotopes to estimate $f$ ?

Our results showed that the  $f$  values of the 15 sites ranged between 11% - 30%, with an average of 21% and a standard deviation of 6%. Previous metadata analysis (while data reported by Schlesinger and Jasechko (2014) as transpiration to evapotranspiration ratio, we modified these values and reported as evaporation to precipitation ratio ( $f$ ); **Fig. 6a**) showed  
250 that  $f$  varied with the mean annual precipitation and had a wide range (9-79%) on the global scale. Our estimates fall within the range of that under similar precipitation region (350-800 mm yr<sup>-1</sup>). In particular, their average values did not differ significantly with ours ( $p>0.05$ ) and are thus comparable to our estimates ( $21 \pm 6\%$  vs  $33 \pm 15\%$ ; **Fig. 6b-c**). We understand that the data presented by Schlesinger and Jasechko (2014) collected from different methods and that the temporal



and spatial scales over which  $f$  is estimated differ among the methods (Sutanto et al., 2014;Kool et al., 2014;Anderson et  
255 al., 2017).

Additionally, we find that  $f$  is poorly correlated to the potential evapotranspiration but increased with the increase in the  
well-known Budyko dryness index while decreased with the increase in average annual precipitation (**Fig. 5**). Our result is  
consistent with Hsieh et al. (1998), who used shallow soil water isotopic compositions to investigate evaporation along an  
arid to humid transect in Hawaii. However, our result differs from the results of Sprenger et al. (2017b), who investigated  
260 evaporation in a boreal catchment in the Scottish Highlands and showed that evaporation is positively correlated with the  
potential evapotranspiration. One possible explanation for the difference is that the energy is limited for water evaporated  
from soil under the wetter and colder climate condition (Budyko dryness index  $< 1$ ), while our sites are more water-limited  
(Budyko dryness index  $> 1$ ) (Roderick and Farquhar, 2011;Good et al., 2017).

#### 4.4 The advantages of using lc-excess to quantitatively estimate $f$

265 We presented a new method—coupling  $f$  with the qualitative indicator of evaporation intensity (lc-excess)—based on the  
Rayleigh fractionation theory, which takes advantage of isotopic fractionation effect between precipitation and soil water  
to estimate  $f$ . Comparing with the well-known Craig-Gordon method (Craig and Gordon, 1965) and the d-excess method  
(Hu et al., 2018;Zhao et al., 2018), our new method has two advantages. First, it does not require the actual stable isotopic  
values of the initial water source, which is an essential parameter for the other two methods. Source water isotopic compo-  
270 sitions are often difficult to determine in the natural water cycle (Skrzypek et al., 2015;Bowen et al., 2018), thus, evapora-  
tion estimates remain an uncertainty. Locally, deep soil water only originates from local precipitation when there is no ir-  
rigation (Cheng et al., 2014), and thus we can assume that the lc-excess of the initial water is zero according to the original  
definition (Landwehr and Coplen, 2006). This simple assumption—the foundation for our new method and valid for most  
regions around the globe—removes the requirement of the difficult-to-obtain isotopic composition of the initial water  
275 source. As a result, our method only needs the parameters (slope and intercept) of LMWL, which can be determined using  
precipitation isotope data at the interest site by monitoring, GNIP (Global Network of Isotopes in Precipitation), and pre-  
cipitation isoscape (Putman and Bowen, 2019). Other isotopes-based method requires also the isotopic composition of the



initial water source, which are rarely available in applications, precluding them from their wide applications around the globe.

280 Another advantage is that our new method links the quantitative  $f$  with lc-excess. As the lc-excess is a more representative indicator of evaporation than the single isotope system ( $^{18}\text{O}$  or  $^2\text{H}$ ) and the d-excess (Sprenger et al., 2017b; Masson-Delmotte et al., 2005), evaporation estimates from the new method should be more accurate. Moreover, similar to the d-excess method (Hu et al., 2018), the new method combines  $^2\text{H}$  and  $^{18}\text{O}$ , avoiding the inconsistency between the separate implementation of  $^2\text{H}$  and  $^{18}\text{O}$  in the Craig-Gordon method (Sprenger et al., 2017a; Mahindawansa et al., 2019). Overall,  $f$  estimation using the new method is more robust than the remaining two methods and would be widely  
285 applicable.

## 5 Conclusions

We obtained deep isotope profiles (up to 10 m) at 15 sites on China's Loess Plateau to validate the possibility of the long-term evaporation to precipitation ratio estimation using deep soil water isotopic compositions (2-10 m). First, we  
290 present a novel method to estimate  $f$  with lc-excess, which, unlike the other commonly-used isotope methods, does not require the difficult-to-obtain isotopic composition of the initial water source. Second, the  $f$  estimated by the new method and deep soil water isotopic compositions varies among sites, ranging from 11% to 30%, with an average of 21% and a standard deviation of 6%. These values represent a long-term average value because deep soil water has a long residence time (years to decades). They are comparable with the previous estimates at annual scale under similar climate regions of  
295 the world. Additionally, over 60% of the variability is explained by the well-known Budyko dryness index while it is poorly correlated to the potential evapotranspiration, possibly because the water supply is the first limit under such a dry climate. The proposed method could improve the  $f$  estimation for regional and global water balance and apportioning precipitation water into evaporation and other hydrological processes.



### Author contribution

300 W. Xiang and B.C. Si designed the research, prepared and interpreted the data, and wrote the manuscript. M. Li and H. Li offered constructive suggestions for the manuscript. W. Xiang and H. Li conducted the fieldwork.

### Competing interests

The authors declare that they have no conflict of interest.

### Acknowledgments

305 This work was jointly funded by the Natural Science Foundation of China (41630860, 41601222, and 41877017), the Fundamental Research Funds for the Central Universities (2452017317), and the 111 Project (No. B12007). The authors thank Qifan Wu, Ze Tao, Keyu Liu, and Wenjie Wu for their help with the soil sampling and isotope analysis and also the editor and reviewers for their valuable comments and suggestions. We greatly appreciate Jingjing Jin for her great support and assistance to the instrument used in this experiment. We thank Jeffrey McDonnell for useful comments on an earlier  
310 version of this paper.

### References

- Allison, G. B., and Barnes, C. J.: Estimation of evaporation from non-vegetated surfaces using natural deuterium, *Nature*, 301, 143-145. doi: 10.1038/301143a0, 1983.
- Allison, G. B., and Hughes, M. W.: The use of natural tracers as indicators of soil-water movement in a temperate  
315 semi-arid region, *Journal of Hydrology*, 60, 157-173. doi: 10.1016/0022-1694(83)90019-7, 1983.
- Anderson, R. G., Zhang, X. D., and Skaggs, T. H.: Measurement and Partitioning of Evapotranspiration for Application to Vadose Zone Studies, *Vadose Zone Journal*, 16, 1-9. doi: 10.2136/vzj2017.08.0155, 2017.
- Benettin, P., Volkmann, T. H. M., von Freyberg, J., Frentress, J., Penna, D., Dawson, T. E., and Kirchner, J.: Effects of climatic seasonality on the isotopic composition of evaporating soil waters, *Hydrol Earth Syst Sc*, 22, 2881-2890. doi:  
320 10.5194/hess-22-2881-2018, 2018.
- Birkel, C., Soulsby, C., and Tetzlaff, D.: Developing a consistent process- based conceptualization of catchment functioning using measurements of internal state variables, *Water Resour Res*, 50, 3481-3501. doi:



- 10.1002/2013WR014925, 2014.
- 325 Bowen, G. J., Putman, A., Brooks, J. R., Bowling, D. R., Oerter, E. J., and Good, S. P.: Inferring the source of evaporated waters using stable H and O isotopes, *Oecologia*, 187, 1025-1039. doi: 10.1007/s00442-018-4192-5, 2018.
- Chen, J. S., Liu, X. Y., Wang, C. Y., Rao, W. B., Tan, H. B., Dong, H. Z., Sun, X. X., Wang, Y. S., and Su, Z. G.: Isotopic constraints on the origin of groundwater in the Ordos Basin of northern China, *Environ Earth Sci*, 66, 505-517. doi: 10.1007/s12665-011-1259-6, 2012.
- 330 Cheng, L. P., Liu, W. Z., Li, Z., and Chen, J.: Study of Soil Water Movement and Groundwater Recharge for the Loess Tableland Using Environmental Tracers, *T Asabe*, 57, 23-30. doi: 10.13031/trans.56.10017, 2014.
- Clark, I. D., and Fritz, P.: *Environmental isotopes in hydrogeology*, CRC Press/Lewis Publishers, Boca Raton, FL, 328 p. pp., 1997.
- Craig, H., and Gordon, L. I.: *Deuterium and Oxygen 18 Variations in the Ocean and Marine Atmosphere*, Symposium on Marine Geochemistry, 1965, 277-374,
- 335 Dansgaard, W.: Stable isotopes in precipitation, *Tellus*, 16, 436-468. 1964.
- DePaolo, D. J., Conrad, M. E., Maher, K., and Gee, G. W.: Evaporation effects on oxygen and hydrogen isotopes in deep vadose zone pore fluids at Hanford, Washington, *Vadose Zone Journal*, 3, 220-232. doi: 10.2136/vzj2004.2200, 2004.
- Evaristo, J., McDonnell, J. J., Scholl, M. A., Bruijnzeel, L. A., and Chun, K. P.: Insights into plant water uptake from xylem-water isotope measurements in two tropical catchments with contrasting moisture conditions, *Hydrol Process*, 30,
- 340 3210-3227. doi: 10.1002/hyp.10841, 2016.
- Fontes, J. C., Yousfi, M., and Allison, G. B.: Estimation of long-term, diffuse groundwater discharge in the northern Sahara using stable isotope profiles in soil water, *Journal of Hydrology*, 86, 315-327. doi: 10.1016/0022-1694(86)90170-8, 1986.
- Gazis, C., and Feng, X. H.: A stable isotope study of soil water: evidence for mixing and preferential flow paths, *Geoderma*, 119, 97-111. doi: 10.1016/S0016-7061(03)00243-X, 2004.
- 345 Gonfiantini, R.: Environmental isotopes in lake studies, in: *The Terrestrial Environment*, in: *Handbook of Environmental Isotope Geochemistry*, edited by: Fritz, P., and Fontes, J. C., Elsevier, Amsterdam, 113-168, 1986.
- Good, S. P., Noone, D., and Bowen, G.: WATER RESOURCES. Hydrologic connectivity constrains partitioning of global terrestrial water fluxes, *Science*, 349, 175-177. doi: 10.1126/science.aaa5931, 2015.
- 350 Good, S. P., Moore, G. W., and Miralles, D. G.: A mesic maximum in biological water use demarcates biome sensitivity to aridity shifts, *Nat Ecol Evol*, 1, 1883-1888. doi: 10.1038/s41559-017-0371-8, 2017.
- Gu, C. J., Ma, J. Z., Zhu, G. F., Yang, H., Zhang, K., Wang, Y. Q., and Gu, C. L.: Partitioning evapotranspiration using an optimized satellite-based ET model across biomes, *Agr Forest Meteorol*, 259, 355-363. doi: 10.1016/j.agrformet.2018.05.023, 2018.
- Horita, J., Rozanski, K., and Cohen, S.: Isotope effects in the evaporation of water: a status report of the Craig-Gordon model, *Isot Environ Healt S*, 44, 23-49. doi: 10.1080/10256010801887174, 2008.
- 355 Hsieh, J. C. C., Chadwick, O. A., Kelly, E. F., and Savin, S. M.: Oxygen isotopic composition of soil water: Quantifying evaporation and transpiration, *Geoderma*, 82, 269-293. doi: 10.1016/S0016-7061(97)00105-5, 1998.
- Hu, Y. D., Liu, Z. H., Zhao, M., Zeng, Q. R., Zeng, C., Chen, B., Chen, C. Y., He, H. B., Cai, X. L., Ou, Y., and Chen, J.: Using deuterium excess, precipitation and runoff data to determine evaporation and transpiration: A case study from the



- 360 Shawan Test Site, Puding, Guizhou, China, *Geochimica Et Cosmochimica Acta*, 242, 21-33. doi: 10.1016/j.gca.2018.08.049, 2018.
- Huang, Y. N., Evaristo, J., and Li, Z.: Multiple tracers reveal different groundwater recharge mechanisms in deep loess deposits, *Geoderma*, 353, 204-212. doi: 10.1016/j.geoderma.2019.06.041, 2019.
- Jasechko, S., Sharp, Z. D., Gibson, J. J., Birks, S. J., Yi, Y., and Fawcett, P. J.: Terrestrial water fluxes dominated by  
365 transpiration, *Nature*, 496, 347-350. doi: 10.1038/nature11983, 2013.
- Jasechko, S., Perrone, D., Befus, K. M., Cardenas, M. B., Ferguson, G., Gleeson, T., Luijendijk, E., McDonnell, J. J., Taylor, R. G., Wada, Y., and Kirchner, J. W.: Global aquifers dominated by fossil groundwaters but wells vulnerable to modern contamination, *Nat Geosci*, 10, 425-429. doi: 10.1038/NGEO2943, 2017.
- Jin, Z., Guo, L., Lin, H., Wang, Y. Q., Yu, Y. L., Chu, G. C., and Zhang, J.: Soil moisture response to rainfall on the  
370 Chinese Loess Plateau after a long-term vegetation rehabilitation, *Hydrol Process*, 32, 1738-1754. doi: 10.1002/hyp.13143, 2018.
- Kool, D., Agam, N., Lazarovitch, N., Heitman, J. L., Sauer, T. J., and Ben-Gal, A.: A review of approaches for evapotranspiration partitioning, *Agr Forest Meteorol*, 184, 56-70. doi: 10.1016/j.agrformet.2013.09.003, 2014.
- Landwehr, J. M., and Coplen, T. B.: Line-conditioned excess: a new method for characterizing stable hydrogen and  
375 oxygen isotope ratios in hydrologic systems, in: In international conference on isotopes in environmental studies, Vienna: IAEA, 132-135, 2006.
- Li, H., Si, B. C., and Li, M.: Rooting depth controls potential groundwater recharge on hillslopes, *J Hydrol*, 564, 164-174. doi: 10.1016/j.jhydrol.2018.07.002, 2018.
- Li, Z., and Si, B. C.: Reconstructed Precipitation Tritium Leads to Overestimated Groundwater Recharge, *J Geophys Res-Atmos*, 123, 9858-9867. doi: 10.1029/2018JD028405, 2018.
- 380 Li, Z., Jasechko, S., and Si, B. C.: Uncertainties in tritium mass balance models for groundwater recharge estimation, *J Hydrol*, 571, 150-158. doi: 10.1016/j.jhydrol.2019.01.030, 2019.
- Lian, X., Piao, S. L., Huntingford, C., Li, Y., Zeng, Z. Z., Wang, X. H., Ciais, P., McVicar, T. R., Peng, S. S., Otle, C., Yang, H., Yang, Y. T., Zhang, Y. Q., and Wang, T.: Partitioning global land evapotranspiration using CMIP5 models  
385 constrained by observations, *Nat Clim Change*, 8, 640-+. doi: 10.1038/s41558-018-0207-9, 2018.
- Lin, G. W.: Study on soil moisture characteristics and its affecting factors for the Baicao loess tableland by using environmental tracers, Master, Northwest A&F University, 2017.
- Lin, H.: Linking principles of soil formation and flow regimes, *Journal of Hydrology*, 393, 3-19. doi: 10.1016/j.jhydrol.2010.02.013, 2010.
- 390 Lin, R. F., and Wei, K. Q.: Tritium profiles of pore water in the Chinese loess unsaturated zone: Implications for estimation of groundwater recharge, *J Hydrol*, 328, 192-199. doi: 10.1016/j.jhydrol.2005.12.010, 2006.
- Liu, T. S.: *Loess and the Environment*, Chian Ocean Presss, Beijing, 1985.
- Mahindawansa, A., Külls, C., Kraft, P., and Breuer, L.: Estimating water flux and evaporation losses using stable isotopes of soil water from irrigated agricultural crops in tropical humid regions, *Hydrology and Earth System Sciences Discussions*,  
395 2019, 1-28. doi: 10.5194/hess-2019-213, 2019.
- Majoube, M.: Fractionnement en oxygène 18 et en deutérium entre l'eau et sa vapeur, *Journal de Chimie Physique et de*





- Physico-Chimie Biologique, 68, 1423-1436. 1971.
- Masson-Delmotte, V., Jouzel, J., Landais, A., Stievenard, M., Johnsen, S. J., White, J. W., Werner, M., Sveinbjornsdottir, A., and Fuhrer, K.: GRIP deuterium excess reveals rapid and orbital-scale changes in Greenland moisture origin, *Science*, 309, 118-121. doi: 10.1126/science.1108575, 2005.
- 400 Niu, Z., He, H., Zhu, G., Ren, X., Zhang, L., Zhang, K., Yu, G., Ge, R., Li, P., Zeng, N., and Zhu, X.: An increasing trend in the ratio of transpiration to total terrestrial evapotranspiration in China from 1982 to 2015 caused by greening and warming, *Agr Forest Meteorol*, 279, 107701. doi: 10.1016/j.agrformet.2019.107701, 2019.
- Or, D., and Lehmann, P.: Surface Evaporative Capacitance: How Soil Type and Rainfall Characteristics Affect Global-Scale Surface Evaporation, *Water Resour Res*, 55, 519-539. 2019.
- 405 Orłowski, N., Breuer, L., and McDonnell, J. J.: Critical issues with cryogenic extraction of soil water for stable isotope analysis, *Ecohydrology*, 9, 3-10. doi: 10.1002/eco.1722, 2016.
- Penman, H. L.: Natural evaporation from open water, bare soil and grass, *Proceedings of the Royal Society of London. Series A, Mathematical and physical sciences*, 193, 120-145. doi: 10.1098/rspa.1948.0037, 1948.
- 410 Putman, A. L., and Bowen, G. J.: Technical note: A global database of the stable isotopic ratios of meteoric and terrestrial waters, *Hydrol. Earth Syst. Sci. Discuss.*, 2019, 1-14. doi: 10.5194/hess-2019-173, 2019.
- Roderick, M. L., and Farquhar, G. D.: A simple framework for relating variations in runoff to variations in climatic conditions and catchment properties, *Water Resour Res*, 47. doi: 10.1029/2010wr009826, 2011.
- Schlesinger, W. H., and Jasechko, S.: Transpiration in the global water cycle, *Agr Forest Meteorol*, 189, 115-117. doi: 415 10.1016/j.agrformet.2014.01.011, 2014.
- Scott, R. L., and Biederman, J. A.: Partitioning evapotranspiration using long-term carbon dioxide and water vapor fluxes, *Geophys Res Lett*, 44, 6833-6840. doi: 10.1002/2017GL074324, 2017.
- Skrzypek, G., Mydlowski, A., Dogramaci, S., Hedley, P., Gibson, J. J., and Grierson, P. F.: Estimation of evaporative loss based on the stable isotope composition of water using Hydrocalculator, *Journal of Hydrology*, 523, 781-789. doi: 420 10.1016/j.jhydrol.2015.02.010, 2015.
- Sprenger, M., Herbstritt, B., and Weiler, M.: Established methods and new opportunities for pore water stable isotope analysis, *Hydrological Processes*, 29, 5174-5192. doi: 10.1002/hyp.10643, 2015.
- Sprenger, M., Leistert, H., Gimbel, K., and Weiler, M.: Illuminating hydrological processes at the soil-vegetation-atmosphere interface with water stable isotopes, *Rev Geophys*, 54, 674-704. doi: 10.1002/2015RG000515, 425 2016.
- Sprenger, M., Tetzlaff, D., and Soulsby, C.: Stable isotopes reveal evaporation dynamics at the soil-plant atmosphere interface of the critical zone, *Hydrology and Earth System Sciences Discussions*, 2017, 1-37. doi: 10.5194/hess-2017-87, 2017a.
- Sprenger, M., Tetzlaff, D., Tunaley, C., Dick, J., and Soulsby, C.: Evaporation fractionation in a peatland drainage network affects stream water isotope composition, *Water Resour Res*, 53, 851-866. doi: 10.1002/2016WR019258, 2017b.
- 430 Stoy, P. C., El-Madany, T., Fisher, J. B., Gentine, P., Gerken, T., Good, S. P., Liu, S., Miralles, D. G., Perez-Priego, O., Skaggs, T. H., Wohlfahrt, G., Anderson, R. G., Jung, M., Maes, W. H., Mammarella, I., Mauder, M., Migliavacca, M., Nelson, J. A., Poyatos, R., Reichstein, M., Scott, R. L., and Wolf, S.: Reviews and syntheses: Turning the challenges of



- partitioning ecosystem evaporation and transpiration into opportunities, *Biogeosciences Discussions*, 2019, 1-47. doi:  
435 10.5194/bg-2019-85, 2019.
- Sutanto, S. J., van den Hurk, B., Dirmeyer, P. A., Seneviratne, S. I., Rockmann, T., Trenberth, K. E., Blyth, E. M.,  
Wenninger, J., and Hoffmann, G.: HESS Opinions "A perspective on isotope versus non-isotope approaches to determine  
the contribution of transpiration to total evaporation", *Hydrol Earth Syst Sc*, 18, 2815-2827. doi:  
10.5194/hess-18-2815-2014, 2014.
- 440 Tan, H., Liu, Z., Rao, W., Wei, H., Zhang, Y., and Jin, B.: Stable isotopes of soil water: Implications for soil water and  
shallow groundwater recharge in hill and gully regions of the Loess Plateau, China, *Agriculture, Ecosystems &  
Environment*, 243, 1-9. doi: 10.1016/j.agee.2017.04.001, 2017.
- Thomas, E. M., Lin, H., Duffy, C. J., Sullivan, P. L., Holmes, G. H., Brantley, S. L., and Jin, L. X.: Spatiotemporal Patterns  
of Water Stable Isotope Compositions at the Shale Hills Critical Zone Observatory: Linkages to Subsurface Hydrologic  
445 Processes, *Vadose Zone Journal*, 12. doi: 10.2136/vzj2013.01.0029, 2013.
- Wan, H., and Liu, W. G.: An isotope study ( $\delta O-18$  and  $\delta D$ ) of water movements on the Loess Plateau of China in  
arid and semiarid climates, *Ecological Engineering*, 93, 226-233. doi: 10.1016/j.ecoleng.2016.05.039, 2016.
- Xu, X. L., and Liu, W.: The global distribution of Earth's critical zone and its controlling factors, *Geophys Res Lett*, 44,  
3201-3208. doi: 10.1002/2017GL072760, 2017.
- 450 Yang, Y. G., and Fu, B. J.: Soil water migration in the unsaturated zone of semiarid region in China from isotope evidence,  
*Hydrol Earth Syst Sc*, 21, 1757-1767. doi: 10.5194/hess-21-1757-2017, 2017.
- Zhang, Z. Q., Evaristo, J., Li, Z., Si, B. C., and McDonnell, J. J.: Tritium analysis shows apple trees may be transpiring  
water several decades old, *Hydrol Process*, 31, 1196-1201. doi: 10.1002/hyp.11108, 2017.
- Zhao, C. L., Shao, M. A., Jia, X. X., Huang, L. M., and Zhu, Y. J.: Spatial distribution of water-active soil layer along the  
455 south-north transect in the Loess Plateau of China, *J Arid Land*, 11, 228-240. doi: 10.1007/s40333-019-0051-4, 2019.
- Zhao, M., Hu, Y. D., Zeng, C., Liu, Z. H., Yang, R., and Chen, B.: Effects of land cover on variations in stable hydrogen  
and oxygen isotopes in karst groundwater: A comparative study of three karst catchments in Guizhou Province, Southwest  
China, *Journal of Hydrology*, 565, 374-385. doi: 10.1016/j.jhydrol.2018.08.037, 2018.
- Zheng, S. K., Si, B. C., Zhang, Z. Q., Li, M., and Wu, Q. F.: Mechanism of rainfall infiltration in apple orchards on Loess  
460 Tableland, China, *Chinese Journal of Applied Ecology*, 28, 2870-2878. 2017.
- Zhu, Y. J., Jia, X. X., and Shao, M. A.: Loess Thickness Variations Across the Loess Plateau of China, *Surveys in  
Geophysics*, 39, 715-727. doi: 10.1007/s10712-018-9462-6, 2018.
- Zimmermann, U., Munnich, K. O., Roether, W., Kreutz, W., Schubach, K., and Siegel, O.: Tracers determine movement of  
soil moisture and evapotranspiration, *Science*, 152, 346-347. doi: 10.1126/science.152.3720.346, 1966.

465



## Figures

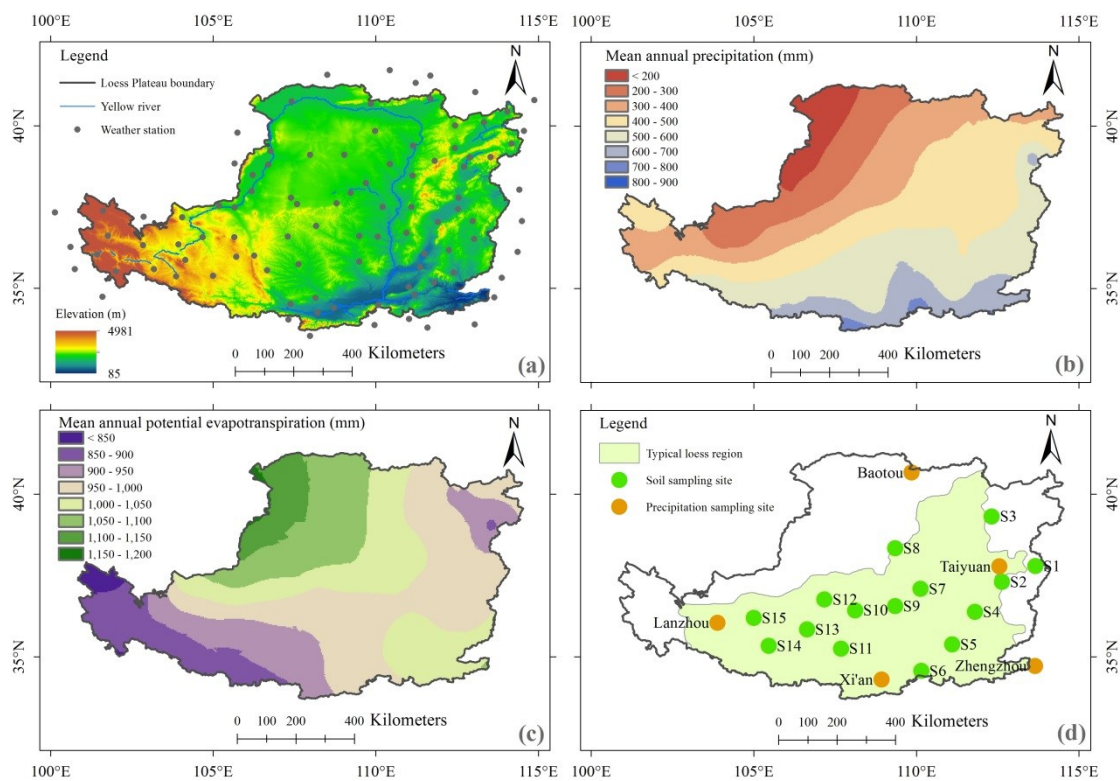
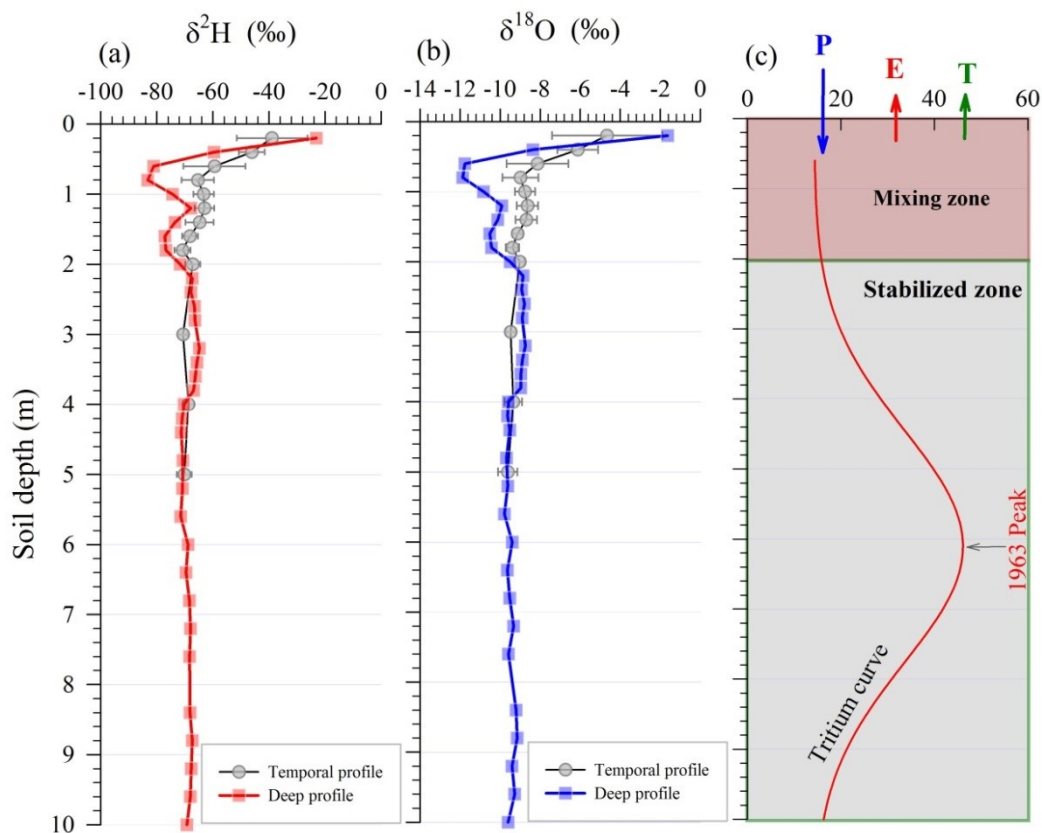


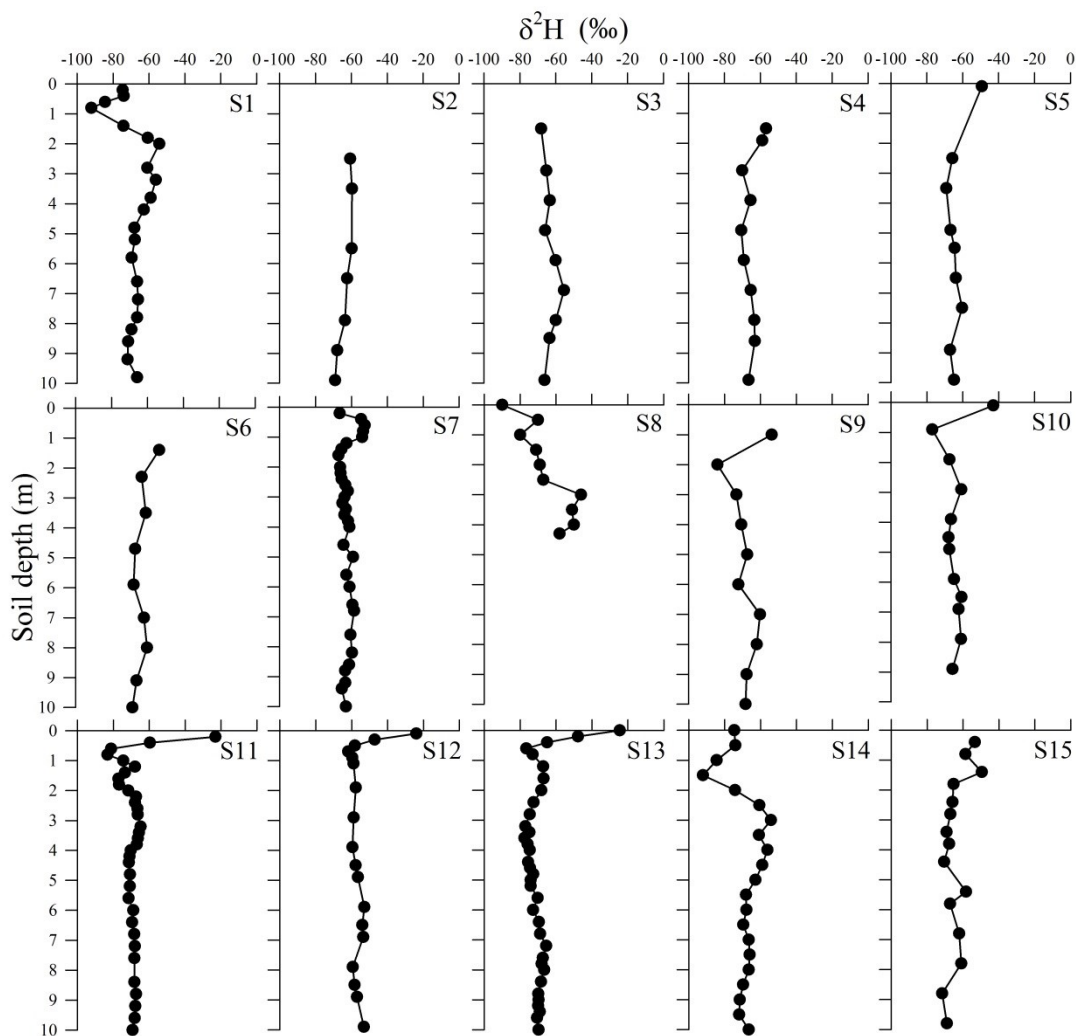
**Figure 1** Spatial patterns of climate and the distribution of the observation sites on China's Loess Plateau. (a) Elevation and weather station; (b) Mean annual precipitation; (c) Mean annual potential evapotranspiration; (d) Soil and precipitation sampling sites.

470



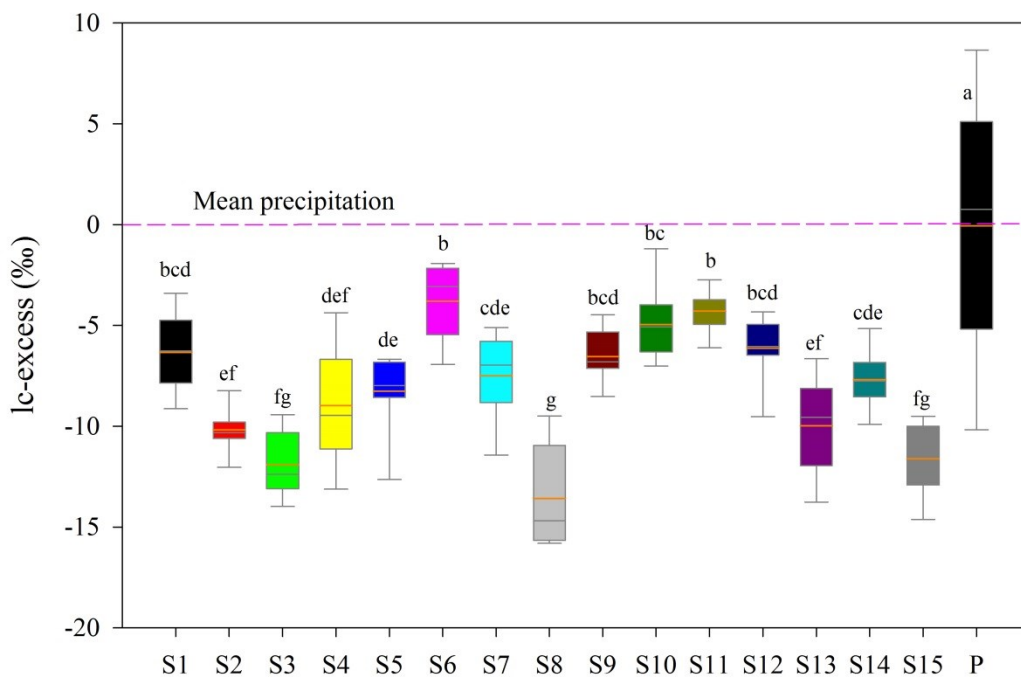
475

**Figure 2** Vertical and temporal distributions of  $\delta^2\text{H}$  (a) and  $\delta^{18}\text{O}$  (b) in soil water at S11 site. The cycle and error bars in (a) and (b) represent mean and one standard deviation from eight repeated measurements between 2015 and 2016. Figure (c) shows that soil profile can be divided into two regions: mixing zone and stabilized zone. Mixing zone represents the top zone where evaporation (E), transpiration (T) and precipitation infiltration (P) occur, and where the evaporation-affected water mixes with new infiltrated precipitation water. A large proportion of the mixed water returns to the atmosphere through evapotranspiration ( $ET = E + T$ ) while a small proportion moves downward into the stabilized zone. The stabilized zone represents the subsurface zone where soil water isotopes no longer exhibit seasonality and are thus depth-invariant. Soil water tritium curve in (d) obtained from the same site is adapted after Li et al. (2018).

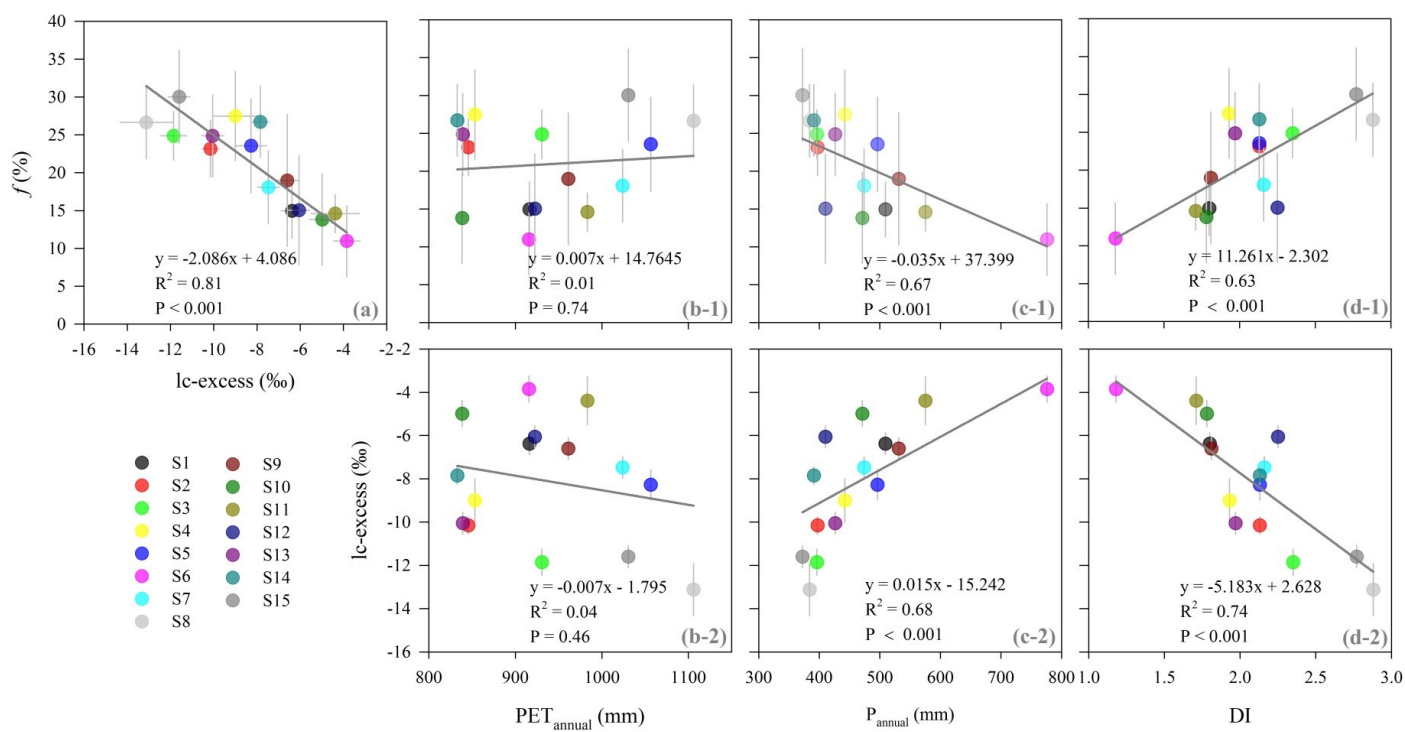


480

**Figure 3** The depth profiles of soil water  $\delta^2\text{H}$  at 15 sites (S1-15) on China's Loess Plateau. Because  $\delta^2\text{H}$  and  $\delta^{18}\text{O}$  strongly covary, here we take  $\delta^2\text{H}$  as an example.



485 **Figure 4** Boxplots of the line-conditioned excess (lc-excess) of precipitation (P) and deep soil water (2 - 10 m) at the 15 sites (S1-15) on China's Loess Plateau. The dashed line represents the mean lc-excess of local precipitation. The boxplots show 10<sup>th</sup>, 25<sup>th</sup>, 50<sup>th</sup>, 75<sup>th</sup>, and 90<sup>th</sup> of lc-excess. The bold orange line stands the average value. Different letters next to the boxplots indicate significant differences according to the post hoc Tukey test ( $\alpha=0.05$ ).



488

489

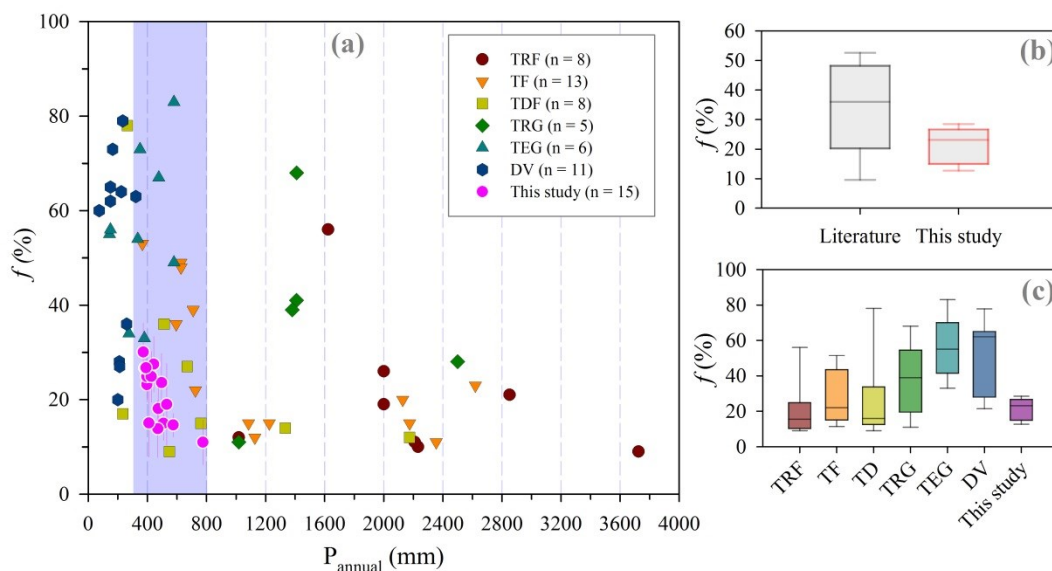
Figure 5 The relationship between evaporation to precipitation ratio ( $f$ ) and deep soil water (2 - 10 m) line-conditioned excess (lc-excess) of 15 sites

490

(S1-15) on China's Loess Plateau (a), and their relation to the annual potential evapotranspiration (PET<sub>annual</sub>), precipitation (P<sub>annual</sub>), and the Budyko

491

dryness index (DI = PET<sub>annual</sub> / P<sub>annual</sub>), respectively (b-d). The gray error bars represent one standard error for each relevant variable.



495 **Figure 6** The evaporation to precipitation ratio ( $f$ ) of this study (farmland or grassland) and previous studies under different  
 vegetation in other climatic zones of the world (data reported by Schlesinger and Jasechko (2014) and here we modified it). (a)  
 The relationship of  $f$  between mean annual precipitation ( $P_{\text{annual}}$ ), and the shadow in the (a) presents the  $P_{\text{annual}}$  range that our  
 estimates coverage (350-800 mm). (b) Comparison of this study with the similar climatic region (shadow coverage). (c) Compar-  
 500 ison of this study with that under different vegetation in other climatic zones of the world. The boxplots in (b)-(c) show 10th,  
 25th, 50th, 75th, and 90th of the  $f$ . In (a), the vertical error bars represent the uncertainties, and TRF, TF, TD, TRG, TEG, DV  
 stands tropical rainforest, temperate forest, temperate deciduous forest, tropical grassland, temperate grassland, and desert  
 vegetation, respectively.





## Tables

**Table 1** General information about soil sampling sites on China's Loess Plateau.

Site	Locations	Latitude	Longitude	Elevation (m)	P (mm)	T (°C)	Rh (%)	PET (mm)	Land use	Soil depth (m)	Data source
S1	Pingding	37.79	113.66	850	509	10.9	55	916	Grassland	10	This study
S2	Taigu	37.30	112.63	1337	397	10.4	58	846	Farmland	10	This study
S3	Suozhou	39.32	112.32	1218	396	7.4	54	931	Farmland	10	This study
S4	Hongtong	36.38	111.80	1004	442	12.7	63	853	Farmland	10	This study
S5	Wenxi	35.38	111.10	640	496	12.9	65	1056	Farmland	10	This study
S6	Qinyu	34.57	110.15	509	776	6.5	62	916	Farmland	10	This study
S7	Qingjian	37.09	110.13	991	474	9.9	59	1024	Grassland	10	This study
S8	Yulin	38.34	109.35	1126	384	8.8	54	1106	-	4.3	Chen et al. (2012)
S9	Yan'an	36.56	109.34	1102	531	9.2	65	961	Grassland	10	This study
S10	Huachi	36.43	108.12	1598	471	8.7	62	838	Farmland	10	This study
S11	Changwu	35.25	107.68	1220	575	9.4	69	983	Farmland	10	This study
S12	Huanxian	36.76	107.17	1415	410	9.2	59	923	Farmland	9	This study
S13	Pengyang	35.84	106.63	1575	426	6.9	61	839	Farmland	10	This study
S14	Tongwei	35.34	105.46	1754	391	7.2	70	833	Grassland	10	Tan et al. (2017)
S15	Huining	36.19	105.00	1803	372	7.3	63	1030	Grassland	10	Lin (2017)

**P, T, and Rh are the long-term (1981-2010) mean annual precipitation, temperature, and relative humidity, respectively. The potential evapotranspiration (PET) calculated using the Penman-Monteith formula (Penman, 1948).**